

Research Articles: Behavioral/Cognitive

# Binding during sequence learning does not alter cortical representations of individual actions

https://doi.org/10.1523/JNEUROSCI.2669-18.2019

Cite as: J. Neurosci 2019; 10.1523/JNEUROSCI.2669-18.2019

Received: 15 October 2018 Revised: 25 June 2019 Accepted: 26 June 2019

This Early Release article has been peer-reviewed and accepted, but has not been through the composition and copyediting processes. The final version may differ slightly in style or formatting and will contain links to any extended data.

Alerts: Sign up at www.jneurosci.org/alerts to receive customized email alerts when the fully formatted version of this article is published.

Copyright © 2019 the authors

### 1 Title:

2 Binding during sequence learning does not alter cortical representations of individual actions 3

### 4 Abbreviated title:

5 Stability of motor representations

### Authors:

- Patrick Beukema<sup>1,2</sup>, Jörn Diedrichsen<sup>3</sup> and Timothy Verstynen<sup>4,2</sup> 8
- 9 <sup>1</sup>Center for Neuroscience, University of Pittsburgh, Pittsburgh, Pennsylvania, 15260
- 10 <sup>2</sup>Center for the Neural Basis of Cognition, University of Pittsburgh & Carnegie Mellon
- 11 University, Pittsburgh, Pennsylvania, 15213
- 12 <sup>3</sup>Brain and Mind Institute, Departments of Statistics & Computer Science, University of Western Ontario
- 13
- 14 <sup>4</sup>Departments of Psychology & Biomedical Engineering, Carnegie Mellon University,
- 15 Pittsburgh, Pennsylvania, 15213

16 17

6 7

### 18 **Corresponding author:**

- 19 Timothy Verstynen
- 20 Department of Psychology
- 21 342C Baker Hall
- 22 Carnegie Mellon University
- 23 Pittsburgh, Pennsylvania, 15213
- 24 email: timothyv@andrew.cmu.edu
- 26 Number of pages: 36
- 27 Number of figures: 6
- 28 Number of tables: 4
- 29

25

- 30 Number of words
- 31 Abstract:
- 32 Introduction:
- 33 Discussion:
- 34 35

### Conflict of interest: None 36

- 37 Acknowledgements: The authors would like to thank Kyle Dunovan and Kevin Jarbo for
- 38 helpful comments on this manuscript. Patrick Beukema received support from the Multimodal
- 39 Neuroimaging Training Program NIH T90 DA022761. This research was sponsored by the
- 40 Pennsylvania Department of Health Formula Award SAP4100062201 and National Science
- 41 Foundation CAREER Award 1351748.

## 42 ABSTRACT

43	As a sequence of movements is learned, serially ordered actions get bound together into sets in
44	order to reduce computational complexity during planning and execution. Here we examined
45	how actions become naturally bound over the course of learning and how this learning impacts
46	cortical representations of individual actions. Across five weeks of practice, neurologically
47	healthy human subjects learned either a complex 32-item sequence of finger movements
48	(Trained group, N=9; 3 female) or randomly ordered actions (Control group, N=9; 3 female).
49	Over the course of practice, responses during sequence production in the Trained group became
50	temporally correlated, consistent with responses being bound together under a common
51	command. These behavioral changes, however, did not coincide with plasticity in the
52	multivariate representations of individual finger movements, assessed using fMRI, at any level of
53	the cortical motor hierarchy. This suggests that the representations of individual actions remain
54	stable, even as the execution of those same actions become bound together in the context of
55	producing a well learned sequence.

### 56 SIGNIFICANCE STATEMENT

57 Extended practice on motor sequences results in highly stereotyped movement patterns that bind 58 successive movements together. This binding is critical for skilled motor performance - yet it is 59 not currently understood how it is achieved in the brain. We examined how binding altered the 60 patterns of activity associated with individual movements which make up the sequence. We 61 found that fine finger control during sequence production involved correlated activity throughout 62 multiple motor regions; however, we found no evidence for plasticity of the representations of 63 elementary movements. This suggests that binding is associated with plasticity at a more abstract 64 level of the motor hierarchy.

### 65 INTRODUCTION

66 Being able to combine simple movements into coordinated sets of actions is critical to 67 many everyday skills, such as typing on the computer or driving a manual transmission car 68 (Lashley, 1951). Over the course of evolution the brain has solved this sequencing problem 69 multiple times, resulting in many interacting algorithms that facilitate the consolidation of 70 complex skills (for review see Beukema and Verstynen 2018). One of these algorithms is the 71 process of set building, also called chunking or binding (Verwey 1996). Binding serial actions 72 into sets improves computational efficiency during the production of complex actions by 73 representing multiple movements under a single selection command (Ramkumar et. al, 2016). 74 To illustrate this process consider the graphical model presented in Figure 1. On each trial, the manual response to a visual cue occurs through a hierarchical system of perception, 75 76 selection (e.g., key), and motor planning (e.g., finger movement), that are all represented as 77 latent states with their own independent sources of noise. In this example, the serial order of cues 78 across trials follows a deterministic sequential order. Prior to training (Figure 1A), each response 79 is selected and planned independently of the other responses. Once the order of cues is learned 80 (Figure 1B), the brain can consolidate the selection process such that a set of motor plans is 81 represented under a single selection state. This selection state is triggered by the presentation of 82 the first stimulus in the series, after which subsequent motor commands are cued by the internal 83 state, rather than by the visual cues. This produces faster responses to items within a set, as well 84 as a correlation in responses within bound sets due to their shared upstream command (Figure 85 1C; Verstynen et al., 2012; Acuna et al., 2014; Lynch et al., 2017).

86

88

### <INSERT FIGURE 1 HERE>

89 Figure 1: The process of response binding A. One each trial, (t), a visual stimulus (s) triggers 90 an appropriate finger response (y), in this case reflecting a response time (RT). In the case of 91 unbound actions, the visual perception (u), selection (w), and motor planning (x) processes are 92 all represented as latent states that operate independently across trials. **B**. With training, the 93 intermediary process of selection binds multiple motor plans together as a set. Each set of 94 actions,  $\tau$ , is triggered by the visual stimulus of the first item in the set. Subsequent actions are 95 then internally triggered, rather than relying on external visual cues. This example shows two 96 bound sets, a three item set followed by a two item set. C. The autocorrelation function of 97 response times for bound actions (dashed line) should exhibit a significant correlation across 98 trials, while unbound actions (solid line) should not exhibit a temporal autocorrelation. **D**. A 99 schematic of four hypothetical voxels in cortical sensory motor networks during the execution of 100 either the index or middling finger, with darker colors reflecting stronger movement-evoked 101 responses. Before training, each finger representation is associated with a unique neural 102 activation pattern. After training, the representations of bound finger movements share more 103 activation and the neural activation patterns are more similar.

104

104	Some forms of non-sequential motor learning rely on the reorganization of movement
106	representations in motor networks (Nudo et. al. 1996), suggesting that action binding during
107	sequence learning could alter internal motor representations of individual movements
108	themselves; however, this effect has been largely unexplored. By examining neural
109	representational patterns, previous work has shown that the structure of individual fingers in
110	primary motor cortex is organized according to their co-articulation during natural hand
111	movements (Ejaz et. al., 2015), suggesting a degree of plasticity of the cortical representations
112	individual digits (Merzenich et al. 1984). Indeed, artificial manipulations of pairwise finger
113	correlations alters the distance between finger representations in primary somatosensory cortex
114	(Kolasinski et. al. 2016), although representations of individual fingers can persist in the cortex
115	even decades after amputation (Kikkert et al. 2016), suggesting some degree of rigidity in
116	sensory areas (Makin & Bensmaia 2017). Thus it remains unclear whether elementary sensory of

of

or

117 motor representations are plastic and subject to changes over time.

118 If individual actions are bound under a common motor command, then the internal 119 representations of those actions, at some level of the motor hierarchy, should change with 120 learning. One possibility is that if two movements are executed repeatedly in a sequence, then 121 the activation of one finger movement may pre-activate the following movement. In the extreme, 122 this model makes the prediction that two fingers that are regularly paired together will become 123 enslaved together over time, thereby reducing behavioral flexibility (Lashley, 1951). This, 124 however, is not typically observed. It is therefore more likely that the process of binding alters 125 the representation of contextually cued actions in upstream regions linked to more abstract 126 response selection (Diedrichsen and Kornysheva, 2015), which would predict observing altered 127 representations in higher premotor areas (e.g., premotor and parietal regions). Wherever this 128 binding process happens, the multivariate activity pattern for the two bound movements should 129 become more similar in that region (Figure 1D). 130 Here we tested this hypothesis using a combination of behavioral analysis and event-

related fMRI. Binding was measured behaviorally by looking at the naturalistic emergence of correlations between successive behavioral responses after training on a unimanual 32-item sequence. Population-level representations of visually-cued single finger movements in the cortex were measured using multivariate analysis of fMRI data both before and after five weeks of training on the complex sequence. If the simple binding hypothesis is correct, then cortical representations for individual actions that are bound should be reduced following prolonged practice at the motor sequence task.

138

### 139 MATERIALS AND METHODS

140 Participants

Eighteen right-handed participants (6 female, mean age: 26 years) were recruited locally from
Carnegie Mellon University (CMU) and the University of Pittsburgh. Two authors (PB and TV)
were included in the sample. All participants provided informed consent and were financially
compensated for their time. All experimental protocols were approved by the Institutional review
board at CMU.

146

# 147 Experimental Design and Statistical Analysis148

149 Participants were trained for 25 nonconsecutive days on a variant of the serial reaction time task 150 (Nissen and Bullemer, 1987). Participants were instructed to train for at least 5 days a week, but 151 could chose to take time off (no more than 2 days) at their discretion, and not in the days leading 152 up to the scan. All experimental procedures were performed on a laptop running Ubuntu 14.04. 153 At the beginning of each training session, participants were instructed to place their right hand 154 over the "h" (index), "j" (middle), "k" (ring), and "l" (pinky) key. Each trial consisted of a 155 presentation of one of four unique fractal cues appearing on a black background. Each cue was 156 uniquely mapped to one of four keys on the keyboard (Figure 2A). The trial ended either when 157 the participant executed a response or once a maximum response window expired, depending on 158 which event happened first. A description of the adaptive response window is presented in the 159 next paragraph. After a trial termination, the next cue was presented after a 250 ms inter-trial 160 interval. Each trial block consisted of 256 trials and was followed by a rest period where the 161 mean response time (RT) and accuracy for that block was provided to the participant. On each 162 training day, participants completed 1792 trials, separated into 7 trial blocks. RT was calculated 163 as the delay between stimulus presentation and a key press. Stimulus presentation and recording

164	was controlled with custom written software in Python using the open source Psychopy package
165	(Peirce, 2007). The software used for training is available on GitHub (CoAxLab, n.d.).
166	Prior to the first session, subjects were assigned to either a Trained group (n=9; 3 female)
167	or a Control group (n=9; 3 female). For participants in the Trained group, trial blocks were
168	separated into two types: blocks of pseudo randomly ordered cues (Random; blocks 1,2,6) or
169	blocks of deterministically ordered cues following an embedded 32-element sequence
170	(Sequence; blocks 3,4,5,7). Figure 2B shows the blockwise structure for a single subject in the
171	Trained group. Trials during the Random blocks were constrained such that repeated
172	presentations of the same cue were excluded. This was done so that Random trial blocks would
173	appear more similar to the Sequence trial blocks. The 32 element sequence presented on
174	Sequence blocks consisted of the following key presses: 3-4-2-3-1-4-2-1-3-4-3-4-1-3-4-2-1-2-4-
175	2-3-1-2-1-2-4-3-1-3-1-2-4 using the mapping (1-index finger, 2-middle finger, 3-ring finger, 4-
176	little finger). Each Sequence block began in a random position of the sequence. For the first 2
177	blocks, the response threshold for each trial was set to 1000 ms. To encourage faster responses,
178	the response window of blocks 3-5 was adaptively controlled such that the response window on
179	one trial block was the mean plus one standard deviation of the RTs from the previous trial
180	block. If that value fell below 200 ms or if the accuracy on the preceding block was less than
181	75%, the threshold was reset to 1000 ms. The threshold was removed for the final probe blocks
182	(6 and 7) so that participants could move as quickly as they chose. For the Control group, the
183	procedure was nearly identical to the Trained group, with the exception that all 7 blocks
184	consisted of pseudorandomly ordered trials, i.e. there was no exposure to Sequence blocks.
185	

186 Analysis of training data

187	Data analysis was conducted with custom python code which is available on GitHub
188	(https://github.com/CoAxLab/binding_manuscript) along with source data to generate all
189	manuscript figures. All behavioral analysis during training focused on responses during the last
190	two trial blocks (probe blocks) when no adaptive response window was applied: Random and
191	Sequence conditions for the Trained group, Random and Random conditions for the Control
192	group. Differences in response time (RT) and accuracy (percent correct responses) were
193	measured as the difference in the means between the last two blocks, normalized by the standard
194	deviation of values in trial block 6, i.e., z-scored difference in performance (Verstynen et al.,
195	2012). In the Trained group this reflects the sequence specific change in performance on each
196	day. Since 3 subjects completed 24/25 days of training, average group visualizations are
197	presented for day 24 so as to evaluate the same state of learning for all subjects.
198	Binding was measured by computing the autocorrelation of the series of RTs within each
199	probe trial block. The first 32 trials were excluded to remove the exponential decay as it distorts
200	the autocorrelation analysis (Verstynen et al., 2012). The linear trend was then removed by
201	regression and the residuals were used to calculate the autocorrelation function for lags 1 through
202	31, following the same procedure as described in (Verstynen et al., 2012; Lynch et al., 2017).
203	Positive autocorrelations could be confounded by the fact that the Trained group executed
204	faster responses than the Control Group. Therefore, we also examined the correlation as a
205	function of the inter-press interval using linear regression. The IPI was computed as the time
206	between successive key presses, and the correlation was computed as before. For every subject
207	we computed the slope of the linear regression line between IPI and correlation (Figure 3D).
208	Since the autocorrelation function measures general associations across all sequential
209	lags, it is not sensitive to specific associations between individual elements, and therefore cannot

9

be used to measure binding between specific finger pairs. Therefore, we conducted a secondary
analysis on the same data but examined pairwise correlations between each distinct element (132) in the sequence across cycles. Average correlations, ordered by sequence element, are shown
in Figure 4A-B. Binding between successive elements is reflected by increases in correlations
before compared to after training.

To measure how much the correlation between finger responses matches the statistical structure of the trained sequence, we collapsed the elementwise correlation matrices by finger identity (index, middle, ring, pinky), forming 4x4 observed correlation matrices. To measure the similarity of the observed binding structure to the expected binding structure, we computed the mean squared error between the finger pairing frequencies of the sequence and observed correlations. This gives a normalized similarity measure for how well the pattern of correlations in the behavioral responses matches the pairwise similarities of the trained sequence.

222

## 223 Imaging acquisition

224 Participants were scanned twice, the day before training started (pre-training) and within 2 days 225 of training completion (post-training). All participants were scanned at the Scientific and Brain 226 Research Center at Carnegie Mellon University on a Siemens Verio 3T magnet fitted with a 32-227 channel head coil. High-resolution T1-weighted anatomical images were collected for 228 visualization and surface reconstruction (MPRAGE, 1 mm isotropic, 176 slices). A fieldmap 229 with dual echo-time images (TR: 746 ms, TE1: 5.00 ms, TE2: 7.46 ms, 66 slices, 2 mm 230 isotropic) was acquired to correct for fieldmap inhomogeneities. For the functional imaging sessions, we acquired 241 T2\* weighted echo-planar imaging volumes (2 mm isotropic, TR: 231 232 2000ms, TE: 30.3 ms, MB factor: 3, 66 slices, A >> P, FoV: 192 mm, interleaved ascending

order, flip angle: 79 deg, matrix size: 96x96x66, slice thickness: 2.00 mm). For the finger
mapping task, we collected a total of 6 runs resulting in 1446 volumes. Functional images were
oriented so as to maximize coverage of the entire cortex and cerebellum. All imaging data is
openly available at OpenNeuro: https://openneuro.org/datasets/ds001233/versions/00003.

237

238 Neuroimaging tasks

239 We collected a set of finger mapping runs to estimate the activation patterns evoked by 240 performing each distinct cue-response pair in isolation (i.e. not embedded within a sequence). 241 Prior to the first scan, subject learned the mapping of cue to effector. The same stimuli from the 242 behavioral experiments were projected on an MR-compatible LCD screen mounted at the rear of 243 the scanner. Participants could see this screen through a mirror mounted on the head coil. 244 Responses were recorded on a five-key MR compatible response glove (PST Inc.) placed under 245 the right hand. Each effector (e.g., individual cue-response pairing) was presented in isolation on 246 each trial with no structured order between trials. Thus, the paradigm only measured responses to 247 individual cued movements, not the sequence itself. Each trial type was repeated 12 times per 248 run totaling 72 trials per session. Subjects were instructed to press the cued key several times 249 following stimulus presentation until the cue disappeared from the screen (1 second). The inter-250 trial interval was sampled according to an exponential distribution ranging from 6-18 seconds. 251 Between runs, subjects were given the option to take several minutes of rest.

252

## 253 Imaging Analysis

Functional imaging data were analyzed using SPM8 (http://www.fil.ion.ucl.ac.uk/spm/) and

255 custom Matlab and Python functions. Raw functional EPI images were realigned to the first

volume. No slice time correction was applied due to the fast TR. These realigned images were
then corrected for field distortions using the field maps. All analyses were performed in native
functional space. Structural T1 images were used to reconstruct the pial and white surfaces using
Freesurfer (Fischl, 2012). All custom code is publicly available (CoAxLab, n.d.).

260 All analyses of task-related responses were performed using a region of interest (ROI) 261 approach. Anatomical ROIs were defined separately for each subject, using the surface based 262 Brodmann areas extracted from Freesurfer (Fischl et al., 2008) following similar conventions as 263 described in (Wiestler and Diedrichsen, 2013). The hand voxels of the primary motor cortex 264 (M1) were defined as the surface nodes with the highest probability of belonging to Brodmann 265 area (BA) 4, 1 cm above and below the hand knob (Yousry et al., 1997). S1 was defined as the 266 nodes in BA1 BA2, BA3a, or BA3b, 1 cm above and below the hand knob. Premotor cortex was 267 defined as the nodes belonging to BA6 medial (PMv) or lateral (PMd) to the medial frontal 268 gyrus. Supplementary motor area (SMA) was defined as the voxels in BA6 along the medial 269 wall. The Freesurfer atlas was used to define the superior parietal gyrus, as well as the putamen 270 and caudate as these regions are not defined by Brodmann areaa. As a control ROI, we extracted 271 the voxels belonging to primary auditory cortex as this region would not be expected to exhibit 272 any significant decoding of the visually-cued finger patterns. Each surface based ROI was projected back into native functional space. 273 274 Analysis for effector representations was performed using representational similarity

analysis (RSA, Kriegeskorte et al., 2008) using the crossnobis estimator (Nili et al., 2014,

276 Walther et al., 2015). A GLM with regressors for each effector was fit for each mapping run,

277 along with the six head motion regressors (x, y, z, pitch, yaw, roll). Omissions and incorrect key

278 presses were regressed out of the model. Raw time series were orthogonalized by eigenvector

279 decomposition and projected into the principal component space to minimize model bias in the 280 decoding. To estimate the differences between finger patterns, we used a cross-validated estimate 281 of the Mahalanobis distance between activity patterns for each effector (Diedrichsen et. al. 282 2016). The "crossnobis" distance has the advantage over other distance measures in that it is 283 unbiased, since noise is orthogonalized across runs, resulting in an expected distance of 0 if a 284 voxel or region does not reliably distinguish two finger patterns (Ejaz et al., 2015). The estimated 285 distance  $(\hat{d}_{i,j})$  between the patterns (u) of two fingers (i,j) was averaged across every pair (m,l)286 of runs (M) resulting in (6 choose 2) = 15 folds using the following equation:

$$\hat{d}_{i,j} = \sum_{l,m;l \neq m}^{M} \frac{(u_i^m - u_j^m)^T (u_i^l - u_j^l)}{M(M-1)}$$

Equation 1

287

Unlike correlation distances, Mahalanobis distances can exceed the value of 1. Furthermore the cross-validated nature of the crossnobis estimate also allows *d* to become negative. The pairwise distances between each of the fingers are summarized in a representational dissimilarity matrix. To test for encoding and plasticity within each voxel or ROI, we extracted the average distance between each pair of fingers pattern (K=4) using the following equation:

$$H = \sum_{i \neq j}^{K} \frac{\hat{d}_{i,j}}{K^2 - K}$$

Equation 2

293

294 To examine the extent of finger representations across all of cortex, we conducted a surface-

295 based searchlight (Oosterhof et al., 2011), assigning every surface node an H value based on the

- 296 local (p=160) patterns surrounding an approximately 10 mm radius. Values for the number of
- 297 voxels (p) and radius were chosen based on previous studies (Yokoi et. al. 2017). This

298 searchlight approach enabled us to examine the entire H distribution across all voxels in each of 299 the ROIs to confirm that each region reliably discriminated individual effectors. Due to the 300 observed positive skew, we extracted the median H for all regions across all subjects and 301 conducted a one sample t-test against 0, in order to establish whether a region reliably decoded 302 the single finger movement representations. 303 Changes in representational distances were estimated by calculating the difference in H 304 values, for each ROI, between the post-training and pre-training imaging sessions (i.e., Hpost-305  $H_{pre}$ ). For each ROI we calculated both pre-training and post-training H values using the responses 306 from all voxels in the region mask. To estimate group-level training effects, the average 307 difference in H from these voxels was calculated for each subject and each ROI. The change in H 308 values was determined by looking for consistent patterns across subjects, within each ROI.

Along with the group level effects, we also calculated the significance of changes in H at thesingle subject level.

In addition to the standard null hypothesis tests, a repeated measures ANOVA was used to examine the influence of training on distances in each ROI. Bayesian repeated measures ANOVA with a JZS prior over all models was used to determine the inclusion Bayes Factor to measure the extent to which the data supported inclusion of the interaction effect (JASP Team, 2017, jasp-stats.org). The guidelines in (Kass and Raftery, 1998) were used to interpret the weight of the evidence in support of the null hypothesis.

317

### 318 RESULTS

319 Learning-related changes in behavior

320	To assess how training impacted performance, we compared the evolution of response times and
321	accuracy across days for the Trained and Control groups. Figure 2B illustrates all trial-wise
322	responses during a single day for a subject in the Trained group. While responses during random
323	trial blocks (black dots) remained relatively constant, the response times during sequence trial
324	blocks (green dots) get steadily faster with training. The last two trial blocks were used to probe
325	learning across time. On average both the Control (dashed line, Figure 2C) and Trained subjects
326	(dashed line, Figure 2D) exhibited a general improvement in response speeds during the final
327	random trial block (block 6). This general across-session speeding of responses during a trial
328	block with random sequences likely reflects the improved learning of the cue-response mapping
329	across days. During the final sequence block (block 7), however, sequence-specific responses in
330	the Trained group also decreased rapidly across training days. Repeated measures ANOVA
331	indicated a significant block x time effect: $F(23,368) = 15.37$ , $p = 7.93 \times 10^{-41}$ , with average
332	response times dropping just below 200ms at the end of training (solid line, Figure 2D). As
333	expected, this effect was not observed in the Control group, $F(23,368) = 0.77$ , $p = 0.76$ , where
334	the final trial block did not contain an embedded sequence (solid line, Figure 2C). In order to
335	capture sequence-specific changes in response speed, we normalized the mean response time for
336	the final trial block (sequence in Trained group, random in Control group) by the mean and
337	variance of response times during trial block 6 (random in both groups; see Methods). This
338	analysis depicts a steady improvement in sequence specific response times across the 5 weeks for
339	the Trained group, with sequence block responses approximately 4 standard deviations faster
340	than the random trial blocks at the end of training (Figure 2E). Repeated measures ANOVA
341	indicated a significant group by time effect, $F(23,368) = 12.79$ , $p = 1.67 \times 10^{-34}$ . Unlike response
342	speed, average accuracy during the final trial block gradually rose at a steady rate for both

345

343 groups, saturating at around 90% for the Trained group and 85% for the Control group, with no

significant between group differences, F(1, 368) = 0.36, p = 0.99 (Figure 2F).

### <INSERT FIGURE 2 HERE>

346 Figure 2: Task design and behavioral performance. A. Participants practiced a serial reaction 347 time task in which each finger movement was prompted by a unique cue. **B**. Representative 348 reaction time plot from Day 12. Each dot represents the response time on one trial. C. Reaction 349 times for the Control group for random trials on blocks 6 and 7. **D**. Reaction times for the 350 Trained group for the random trials (block 6) and sequence trials (block 7). E. Mean z-scored 351 reaction times as a function of day for the Control group (blue) and Trained group (peach). F. 352 Mean accuracy (correct trials/total trials) in the final trial block, as a function of day, for the 353 Control group (blue) and Trained (peach) group. Shaded regions in panels C-F show standard 354 error. 355 356 There are several ways that responses could get faster during the sequence blocks (see

357 Beukema and Verstynen, 2018). The binding hypothesis (Figure 1B), however, makes the

358 specific prediction that serially successive actions that are bound under a shared motor plan

359 should exhibit a correlation in their responses over time, as a consequence of arising from a

360 common, high-level motor plan (Figure 1C). For an index of binding, we used the

361 autocorrelation of RTs during the last trial block for both groups (Verstynen et. al. 2012). Figure

362 3 shows the autocorrelation functions for early (Day 1), middle (Day 12), and late (Day 24)

363 stages of practice for the Control (Figure 3A) and Trained (Figure 3B) groups separately. While

364 participants in the Control group did not show reliable autocorrelation structure in RTs with

365 training, we did see evidence of an emergent structure in the Trained group. Specifically,

366 participants in the Trained group showed no evidence of an autocorrelation in their RTs at Day 1;

367 however, by the middle of training a pronounced autocorrelation of temporally adjacent

368 responses emerged. This correlation increased throughout the training period, tapering off at

approximately the middle of training (Day 12) (Figure 3B inset).

370 To exclude the possibility that the observed increases in RT autocorrelations are simply 371 the result of executing faster responses, we also examined the correlations in consecutive inter-372 trial RTs as a function of inter-press interval (IPI). If the increased correlation in temporally 373 adjacent RTs was simply the result of faster responses, then a negative relationship should exist 374 between the observed autocorrelation and the inter press interval, with higher correlations for 375 faster responses, and little or no correlation for slower responses. A representative example of 376 the relationship between the IPI and the RT correlation is shown in Figure 3C reveals no clear 377 association. Across all subjects, the slope of the regression line between the two variables was 378 not significantly different from zero (Figure 3D). This result suggests that the observed increases 379 in correlation are due to executing responses under a shard motor command and not the result of 380 speed increases alone.

381 We next set out to examine the structure of the associations across movements by 382 examining the pairwise correlations between items in the sequence. For this analysis we 383 organized the data into a matrix of 32 responses by cycles. We then looked at the correlations 384 between different sequence elements across cycles of sequence production. Before practice, this 385 32x32 correlation matrix does not show much structure, with all items approximately equally 386 correlated (Figure 4A). After training, a clear structure in the correlations emerged, with local 387 clusters of correlated responses found along the diagonal of the matrix (Figure 4B). 388 If these clusters of correlated responses in the sequence reflected the inter-finger 389 transition frequency (Figure 4C), then the pairing frequency of individual fingers should 390 determine the degree of similarity between finger responses. Thus we repeated our inter-item 391 correlation analysis, except rather than mapping response to each item in the sequence, we 392 mapped it to the finger that executed the response. This was done by creating a new matrix of

393

394 cycle through the sequence and then calculating the 4x4 correlation matrix of inter-finger 395 responses. The similarity between the observed correlations and expected correlations based on 396 the pairwise frequencies (Figure 4D) was computed using the mean squared error (MSE). The 397 mean observed correlation matrix across all subjects on the final day of training is shown in 398 Figure 4E. There was increased similarity between the observed and expected correlations across 399 days (Figure 4F) in the Trained group F(23,184)=0.0026, but the structure in the Control group 400 remained unchanged F(23,184)=0.41, resulting in a significant group by time interaction, 401 F(368,23) = 1.90, p = 0.0079. These results indicate that binding occurs in a principled way that 402 originates at least in part in the statistical structure of the sequence. 403 <INSERT FIGURE 3 HERE> 404 Figure 3: Binding in behavioral responses. A,B Mean autocorrelation function for lags 1-31 405 during early (day 1, purple), middle (day 12, cyan) and late training (day 24, black) for the 406 Control group (A) and Trained group (B). The asterisks indicates the significant lags, at a cut-off 407 (p < 0.05), for the final training day. Inset in B shows the lag 1 correlation as a function of day 408 for the Trained group. Shaded regions show standard error of the mean. C. Representative 409 correlations as a function of the inter press interval showing that the correlation does not appear 410 to be a function of executing faster responses. D. Boxplots showing the slopes of the linear 411 regression lines from the correlation by IPI relationship depicted in C for each of the Trained 412 subjects on the sequence trials (seq) and the random trials (ran) 413 414

single trial response times with each column representing a finger and each row representing a

### <INSERT FIGURE 4 HERE>

417 418 Figure 4: A,B. Average correlation between each element in the sequence during the final trial 419 block for the Trained group, during Day 1 (A) and Day 24 (B). C. The 32 element sequence 420 showing frequency of each finger transition (i-index, m-middle, r-ring, l-little) F. Pairwise 421 frequencies between each finger **D**. Average observed correlations between fingers at the end of 422 training collapsed across subjects. E. The MSE between the pairwise frequencies (panel F) and 423 observed correlation matrix computed separately for each subject. Smaller numbers indicate 424 increased similarity to the expected pairwise frequencies (F). Shaded regions show standard 425 error.

426 427

### 428 Stable motor representations after training.

429	In order to directly measure multivariate cortical representations of the individual cued
430	movements, we used a rapid-event-related fMRI design consisting of presentations of each cued
431	finger press followed by a period of fixation (Figure 5A). An ROI analysis was performed on the
432	cortical motor network including primary motor cortex, M1; primary somatosensory cortex, S1;
433	dorsal premotor cortex, PMd; ventral premotor cortex, PMv; supplementary motor area, SMA;
434	and the superior parietal lobule, SPL. These regions were anatomically localized using
435	Brodmann areas extracted from Freesurfer (see Materials and Methods). These regions are
436	shown on the group average surface (Figure 5C). In each of the cortical motor ROIs, we
437	quantified the activity pattern related to each cued finger movement and then calculated a cross-
438	validated Mahalanobis (crossnobis) distance between the activity patterns for each cued finger
439	pair (Figure 5B). If two cued fingers generate the same cortical activity patterns, then the
440	corresponding distance between them will be 0. However, if two finger movements consistently
441	generate dissimilar finger patterns, then the corresponding distance will be positive. Cross-
442	validation allows us to test the value of the distance estimates directly against zero (Diedrichsen
443	and Kriegeskorte 2017, Walther et. al. 2016, Diedrichsen et. al. 2016). The distances between
444	every possible pair of fingers is summarized in a representational dissimilarity matrix (RDM) for
445	each ROI (Figure 5D).
446	While the magnitude of the representational distances is slightly smaller than distances

447 reported in previous studies (Ejaz et. al. 2015), likely due to the use of an event-related design in 448 our study, the relative representational patterns that we observed in primary motor and primary 449 somatosensory cortex qualitatively matches previous reports. Specifically the index finger is 450 furthest from the little finger, while the middle and ring fingers are close together. This pattern of

451	representational distances is also similar to what is observed in the other cortical motor regions,
452	although the overall between effector distances are smaller in these premotor regions (Figure
453	5D). To confirm that each region has reliably different representations for the fingers, we
454	computed the average cross-validated pairwise distance between all finger movements (Figure
455	5B see Materials and Methods). Average distance (H) greater than 0 indicate above-chance
456	encoding (Diedrichsen and Kriegeskorte 2017). In order to estimate the reliability of this
457	encoding across subjects, we extracted the median distance across voxels within each searchlight
458	for each subject and ROI. The median was chosen in order to account for the fact that the
459	distribution of H values within a region is highly skewed. A one-sample t-test on those median
460	values (one median per subject), after adjusting for multiple comparisons using a Bonferonni
461	correction, found significant separation of cued finger representations (i.e., positive average
462	distances) in the cortical sensorimotor areas, but not the A1 control region nor the putamen
463	(Table 1). A follow up paired samples t-test (within subject) showed that H was greater in M1,
464	S1, PMd, PMv, and SPL, but not in SMA, when compared against A1 (Table 1).
465	Along with the cortical regions, we also examined the distances between finger
466	representations within the caudate and the putamen (inset of Figure 4E). Overall the distances
467	within the striatum were significantly separable within the caudate but not the putamen.
468	However, the magnitude of the representational distances was very weak in these subcortical
469	regions, with distances several orders of magnitude smaller than in any cortical regions.
470	Overall, the analysis of cortical representations of individual fingers is consistent with
471	previous studies (Ejaz et. al. 2015), confirming that the patterns of activity in the motor network
472	can reliably discriminate individual effectors. This effect is substantially weaker in subcortical
473	regions, likely having to do with the lower signal-to-noise of the BOLD signal in the striatum

474 and other regions of the basal ganglia. Therefore, these regions of interest were excluded from

475 further analysis.

476 477

### <INSERT FIGURE 5 HERE>

478 Figure 5: Multivariate activity patterns during cued finger movements. A. fMRI task schematic. 479 Participants executed single finger movements on the button glove following a variable period of 480 fixation. The cue-finger mapping was identical to that used during the training. B. Example of a 481 representational dissimilarity matrix showing similar finger patterns that result in small 482 distances and dissimilar finger patterns that result in large distances. The average crossnobis 483 similarity (i.e., H) was used as a test statistic for assessing decoding in each ROI and for 484 assessing representational plasticity. C. Regions of interest masks overlaid in blue on the group 485 average surface. D. Average representational dissimilarity matrices for each region. Each 486 colored square within the RDM indicates the distance between those two fingers (i=index, 487 m=middle, r=ring, l=little) **E**,**F**. Violin plots show the distributions of median H values in 488 cortical motor areas (E) and the striatum (F) across subjects. Black circles inside plots show 489 individual data. Asterisks indicate significance at  $\alpha = 0.05$  after correcting for multiple 490 comparisons (Bonferonni). Primary motor cortex (M1), primary somatosensory cortex (S1), 491 premotor dorsal cortex (PMd), premotor ventral cortex (PMv), superior parietal lobule (SPL), 492 supplementary motor area (SMA), and primary auditory cortex (A1), caudate (Cau), putamen 493 (Put).

494 495 To determine whether the emergence of binding in the behavioral responses coincides 496 with alterations of these representational distances of individual cued actions, we measured how 497 average distances changed for each cortical motor ROI before and after training. The simple 498 form of the binding hypothesis is that the representations of frequently paired actions will 499 become more similar (Figure 1D) after training, predicting that the distances between frequently 500 paired movements will decrease after practice only in the Trained group. When looking at all 501 pairwise distances (Figure 6A) we were unable to find a reliable influence of sequence training 502 on the average pattern distances in any cortical motor region. In most areas, the distances

503 decreased only marginally for both Trained and Control groups together, but the finger patterns

504 remained largely separable, with patterns exhibiting a high degree of stability. Across all regions,

505 we failed to detect a reliable interaction between group and time that would be indicative of a

507 order to evaluate the evidence in support of the null hypothesis that the interaction is not present, 508 we conducted a JZS Bayes Factor (BF) ANOVA with uniform prior across all models and found 509 evidence in support of the null model that training does not influence distances. The BF's ranged

training effect in representational distances (all p>0.26, full statistics reported in Table 2). In

510 from 0.099-0.658 (Table 2), which can be considered positive anecdotal evidence in support of

511 the Null hypothesis (Kass & Raftery, 1995).

512

523 524 525

506

### 513

### <INSERT FIGURE 6 HERE>

514 Figure 6: Stable representational distances after training. A. Pairwise finger distances included 515 in overall distance analysis. **B**. Bar plots show mean ROI H values in the pre- and post-training 516 scans separately for each group. Error bars show standard error. Gray circles are individual 517 data points. C. Finger pair frequencies were asymmetrically distributed in the trained sequence 518 (see Figure 4D). Some finger pairs, e.g. index and little were infrequently paired, whereas other 519 finger pairs e.g. index and middle were frequently paired. **D**,**E**. Bar plots show mean H for 520 frequent pairs B (D) and infrequent pairs (E) in the pre- and post-training scans separately for 521 each group. Error bars show standard error. Circles are individual data points. No comparison 522 was found to be statistically significant at  $\alpha = 0.05$ .

Of course, looking at changes in overall representational distances may not be sensitive

526 enough to pick up changes in the representational distances of only a few finger pairs. The

527 simple plasticity model we proposed in the Introduction predicts that the greatest plasticity

528 should be observed in the finger pairs most often executed together in the sequence. If the

529 distances decreased for the more frequently paired effectors, but increased for the less frequently

530 paired effectors this may result in a net change for the overall average distance near 0. To

531 explore this possibility, we re-analyzed the distance changes by looking at the frequently and

532 infrequently occurring finger pairs in the sequence structure itself (Figure 4C). Based on the

533 pairing frequencies, we identified four frequently used finger pairs (index-middle, index-ring,

534 middle-little, ring-little) and two infrequently used pairs (Figure 6C) (middle-ring and index-

535 little). Qualitatively, the pattern of distances for each pair type appeared to match what was 536 observed in the overall distance patterns, with higher distances in M1 and S1, and lower 537 distances in the premotor and parietal regions. Thus, much like the overall distance patterns, we 538 were unable to resolve focal changes in representational distances in either of the most frequently (Figure 6D) or infrequently (Figure 6E) paired effectors. Across all regions, two-way repeated 539 540 measures ANOVA indicated no significant group-by-time interaction for either frequently paired 541 (all p > 0.26, full statistics provided in Table 3) or infrequently paired fingers (all p > 0.13, full 542 statistics provided in Table 4). The Bayesian ANOVA revealed anecdotal evidence in favor of 543 the null hypothesis for both the frequently (BFs: 0.108-0.631, Table 3) and infrequently (BFs: 544 0.108-0.391, Table 4) paired fingers.

545 546

### 547 DISCUSSION

548 Here we examined whether the binding of serial actions during long-term sequence learning 549 alters the cortical representations of individual cue-response pairings. We found that during 550 sequence production, temporally adjacent responses develop a high degree of correlation in their 551 response speeds, consistent with participants binding multiple responses together under a unified 552 command so as to reduce computational complexity (see also Verstynen et. al. 2012, Ramkumar 553 et. al. 2016, Lynch et. al. 2017). Using a multivariate pattern analysis approach, based on the 554 cross-validated Mahalanobis estimator, we also replicated previous studies showing that cortical 555 motor areas reliably distinguish between activation patterns of individually cued finger responses 556 (Ejaz et. al. 2015). We were, however, unable to find evidence for learning-related changes in 557 this representational structure of cued finger responses in any of the cortical regions tested. 558 Taken together, these findings show that the process of binding actions into chunked sets during

long-term skill learning does not impact the representation of individual cued actions, suggesting
that binding relies on changing more complex levels of representation beyond individual
movements.

562 At first glance, the absence of plasticity in population level representations of individual 563 actions that we observed appears to be incompatible with previous reports of plasticity in 564 sensorimotor cortex. Kolansinki and colleagues (2016) found that the representational distances 565 of individual fingers shifted in S1 after physically yoking two fingers together for a period of 24 566 hours. In their study, the sensory representations of the two yoked fingers remained spatially and 567 temporally identical, however the unyoked fingers altered their distances, suggesting a possible 568 compensatory effect in the sensory representations themselves. In contrast to this observation, 569 other papers have shown that finger representations in S1 are still robust and distinct even 570 decades after amputation (Kikkert et al., 2016), suggesting that the sensory representations of 571 digits have some a degree of robustness. In contrast to these sensory representation studies, our 572 task here relied on training associations between temporally independent movements in a 573 specific context. It is possible that, had we trained on chord-like movements, where multiple 574 fingers are simultaneously engaged (Verstynen et. al. 2005), for a longer period of time, we 575 might have observed similar changes in cortical sensorimotor representations, a hypothesis that 576 is left open to future studies.

Alternatively, there is a strong rationale for why single effector representations would remain stable in cortical sensorimotor networks, particularly motor execution areas like M1, after long-term sequence learning. First, binding responses at the execution level may be a maladaptive strategy for maintaining a flexible movement repertoire (Lashley, 1951). For example, if index finger movements were consistently bound with middle finger movements

582 because a single daily task required them to work together in sequential fashion, then they might 583 exhibit a prepotent response in inappropriate contexts. In order to maximize flexibility, it would 584 be beneficial for the movements to be bound at a more abstract motor planning stage, upstream 585 from execution processes. Second, practice may involve refining the control of execution-level 586 representations without necessarily impacting the representations themselves. This would 587 suggest that the process of binding during the consolidation of complex movement sequences is 588 dependent on plasticity mechanisms at hierarchically higher level of processing (Wong et. al. 589 2015).

590 Of course, it is possible that there is plasticity in the representations of individual 591 sensorimotor effectors during long-term sequence learning, but limitations in our experimental 592 design may preclude identifying those changes. First, while the duration of training we used was 593 longer than many classic sequence learning experiments in humans, five weeks may still not be 594 enough time to lead to measurable representational changes in primary motor cortex. This 595 concern is tempered by the fact that we were able to show strong evidence of action binding in 596 the behavioral responses. A second methodological limitation is the lack of power to observe 597 what is likely a relatively modest effect size. Previous studies of sensory representational 598 plasticity provide a reasonable measure of the true effect size, suggesting we are reasonably 599 powered (Kolasinski, 2016). While, it is true that the number of samples was comparatively low 600 for a typical univariate functional imaging study (at 9 participants per group), several design 601 choices alleviate this concern. We collected a substantial amount of data per subject. Each 602 subject was scanned for approximately 2 hours before training, and 2 hours after training, with 6 603 identical and independent imaging sessions per run. This relatively large volume of data per 604 subject enabled us to obtain robust estimates of the population patterns of interest. Thus, while

the number of subjects was modest, we do not believe that our results are simply the result ofinsufficient power.

607Despite these limitations, our experiment clearly shows that five weeks of training on a608complex unimanual sequence task does not alter the sensorimotor representations of individual609effectors despite clear evidence of binding in the motoric actions. This suggests that execution610level representations remain stable during learning and that proficiency is likely controlled by a611higher level within the motor hierarchy.

613

Region	Mean	t(17) H>0	p-value H>0	95% CI (low, high)	t(17) H>H <sup>A1</sup>	p-value H>H <sup>A1</sup>
M1	4.92	7.91	*2.11 x 10 <sup>-7</sup>	3.61, 6.23	7.10	*8.89 x 10 <sup>-7</sup>
S1	5.23	10.13	*6.42 x 10 <sup>-9</sup>	4.14, 6.32	9.40	*1.90 x 10 <sup>-8</sup>
PMd	1.07	5.30	*2.91 x 10 <sup>-5</sup>	0.64, 1.49	3.02	*0.0037
PMv	1.66	12.06	*4.60 x 10 <sup>-10</sup>	1.37, 1.95	4.80	*8.29 x 10 <sup>-5</sup>
SMA	0.57	4.08	*3.87 x 10 <sup>-4</sup>	0.28, 0.87	-0.006	0.49
SPL	1.57	8.44	*8.71 x 10 <sup>-4</sup>	1.18, 1.97	5.13	*4.13 x 10 <sup>-5</sup>
CAU	0.005	3.46	0.0014	0.002, 0.008	-2.75	0.0067
PUT	0.003	1.98	0.031	-0.0002, 0.007	-2.77	0.0065
A1	0.57	2.78	6.45 x 10 <sup>-3</sup>	0.14, 1.01	n.a.	n.a.

614

**Table 1**: T-statistics, and associated p-values testing whether H is significantly greater than 0

(H>0) and whether H is significantly greater than in the control region (H>H<sup>A1</sup>). \* indicates

616 significance based on a Bonferroni corrected threshold (0.05/9) in order to control the family

617 wise error rate.

### 619

Region	F(1,16)	p-value	Inclusion BF
M1	1.820	0.214	0.161
S1	0.069	0.800	0.141
PMd	0.492	0.503	0.099
PMv	1.673	0.232	0.658
SMA	5.092	0.054	0.182
SPL	0.004	0.950	0.145

620 **Table 2:** F-statistics and p-values for testing significance of interaction effect (group x time)

621 from repeated measures ANOVA for mean distances. Inclusion Bayes Factor (BF) is the ratio of

622 the posterior over the prior probability of the model including the interaction term.

624

Region	F(1,16)	p-value	Inclusion BF
M1	1.585	0.243	0.196
S1	0.030	0.867	0.208
PMd	0.089	0.773	0.108
PMv	1.914	0.204	0.631
SMA	6.440	0.035	0.309
SPL	0.001	0.971	0.125

625 *Table 3*: *F* statistics and *p*-values for testing significance of interaction effect (group x time)

626 from repeated measures ANOVA for frequently paired fingers. Inclusion Bayes Factor (BF) is

627 the ratio of the posterior over the prior probability of the model including the interaction term.

628

630

Region	F(1,16)	p-value	Inclusion BF
M1	1.744	0.223	0.135
S1	1.265	0.293	0.218
PMd	1.718	0.226	0.108
PMv	0.708	0.425	0.391
SMA	0.309	0.593	0.149
SPL	0.036	0.854	0.183

631 **Table 4:** F statistics and p-values for testing significance of interaction effect (group x time)

632 from repeated measures ANOVA for the infrequently paired fingers. Inclusion Bayes Factor

(BF) is the ratio of the posterior over the prior probability of the model including the interactionterm.

635

636

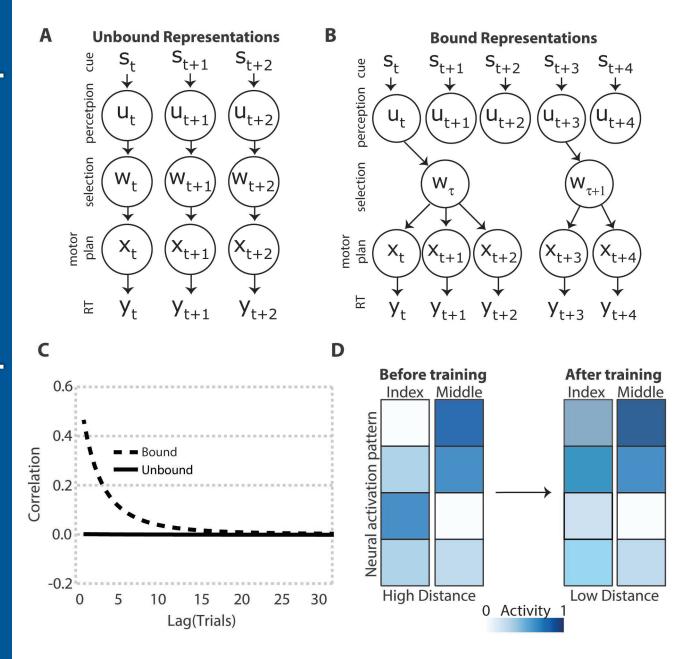
### 638 References

639 640 641	Acuna D.E., Wymbs N.F., Reynolds C.A., Picard N, Turner R.S., Strick P.L., Grafton S.T., Kording K (2014) Multi-faceted aspects of chunking enable robust algorithms. <i>Journal of</i> <i>neurophysiology</i> , 112(8), 1849–1856.
642 643	Beukema P, Verstynen T. (2018). Predicting and Binding: interacting algorithms supporting the consolidation of sequential motor skills. <i>Current Opinion in Behavioral Sciences</i> 20:98-103
644 645	CoAxLab (n.d.) CoAxLab/binding_manuscript: source data and code for stable representations manuscript. Available at: https://github.com/CoAxLab/binding_manuscript
646 647 648 649	Diedrichsen, J., & Kriegeskorte, N. (2017). Representational models: A common framework for understanding encoding, pattern-component, and representational-similarity analysis. <i>PLoS computational biology</i> , <i>13</i> (4), e1005508.
650 651 652	Diedrichsen, J., & Kornysheva, K. (2015). Motor skill learning between selection and execution. <i>Trends in cognitive sciences</i> , 19(4), 227-233.
653 654 655	Diedrichsen, J., Provost, S., & Zareamoghaddam, H. (2016). On the distribution of cross- validated Mahalanobis distances. arXiv preprint arXiv:1607.01371.
656 657	Ejaz N., Hamada M., & Diedrichsen J. (2015) Hand use predicts the structure of representations in sensorimotor cortex. <i>Nature Neuroscience</i> 18(7), 1034-1040.
658	Fischl B. (2012). FreeSurfer. Neuroimage 62:774–781.
659 660 661	Fischl B., Rajendran N., Busa E., Augustinack J., Hinds O., Yeo B.T., Mohlberg H., Amunts K., & Zilles K (2008) Cortical folding patterns and predicting cytoarchitecture. <i>Cerebral Cortex</i> 18(8), 1973–1980.
662 663	JASP Team (2017). JASP (Version 0.8.4). Retrieved from https://jasp-stats.org/
664 665 666	Jin, X., Tecuapetla, F., & Costa, R. M. (2014). Basal ganglia subcircuits distinctively encode the parsing and concatenation of action sequences. <i>Nature neuroscience</i> , 17(3), 423-430.
667 668 669	Kass, R. E., & Raftery, A. E. (1995). Bayes factors. Journal of the american statistical association, 90(430), 773-795.
670 671 672	Kikkert, S., Kolasinski, J., Jbabdi, S., Tracey, I., Beckmann, C. F., Johansen-Berg, H., & Makin, T. R. (2016). Revealing the neural fingerprints of a missing hand. <i>Elife</i> , <i>5</i> , e15292.
673	Kolasinski, J., Makin, T. R., Logan, J. P., Jbabdi, S., Clare, S., Stagg, C. J., & Johansen-Berg, H.
674	(2016). Perceptually relevant remapping of human somatotopy in 24 hours. Elife, 5, e17280.
675	

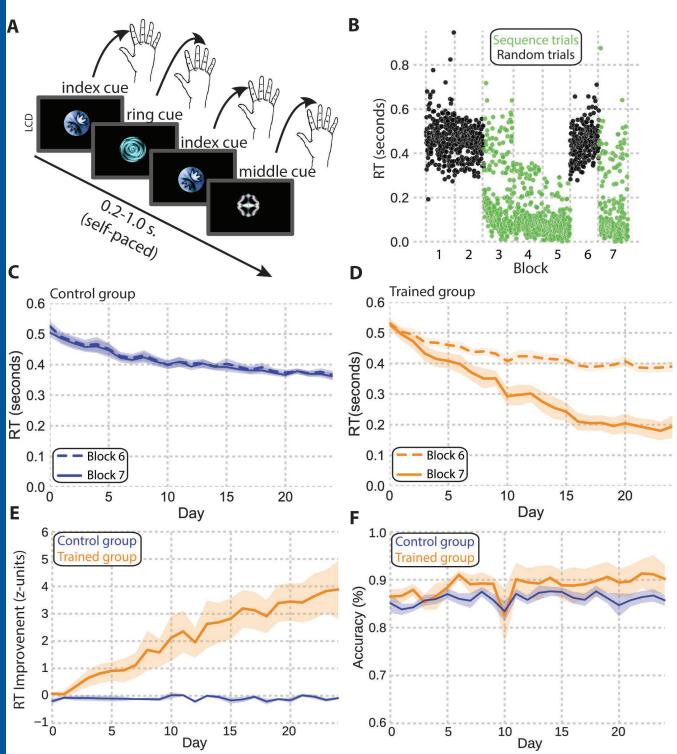
- Kriegeskorte N., Mur M., Bandettini P. (2008). Representational similarity analysis connecting
   the branches of systems neuroscience. *Frontiers in systems neuroscience* 2.
- Lashley, K.S. (1951). The problem of serial order in behavior. In: *Cerebral mechanisms in behavior*, pp 112–136.
- Lynch B., Beukema P., Verstynen T. (2017). Differentiating Visual from Response Sequencing
   During Long-term Skill Learning. *Journal of cognitive neuroscience* 29(1), 125–136.
- Makin, T. R., & Bensmaia, S. J. (2017). Stability of sensory topographies in adult cortex. *Trends in cognitive sciences*, 21(3), 195-204.
- Merzenich, M. M., Nelson, R. J., Stryker, M. P., Cynader, M. S., Schoppmann, A., & Zook, J.
   M. (1984). Somatosensory cortical map changes following digit amputation in adult monkeys. *Journal of comparative Neurology*, 224(4), 591-605.
- Nili H., Wingfield C., Walther A., Su L., Marslen-Wilson W., Kriegeskorte N. (2014). A toolbox
   for representational similarity analysis. *PLoS computational biology* 10(4):e1003553.
- Nissen M.J., Bullemer P. (1987). Attentional requirements of learning: Evidence from
   performance measures. *Cognitive psychology*, 19(1), 1–32.
- Nudo R.J., Milliken G.W., Jenkins W.M., Merzenich M.M. (1996). Use-dependent alterations of
   movement representations in primary motor cortex of adult squirrel monkeys. *Journal of Neuroscience*, 16(2), 785–807.
- Oosterhof N.N., Wiestler T., Downing P.E., Diedrichsen J. (2011). A comparison of volume based and surface-based multi-voxel pattern analysis. *Neuroimage*, 56(2), 593–600.
- Peirce J.W. (2007). PsychoPy-Psychophysics software in Python. *Journal of neuroscience methods*, 162(1), 8–13.
- Ramkumar P., Acuna D.E., Berniker M., Grafton S.T., Turner R.S., Kording K.P. (2016)
   Chunking as the result of an efficiency computation trade-off. *Nature communications*, 700 7:12176.
- Verstynen T., Diedrichsen J., Albert N., Aparicio P., Ivry R.B. (2005). Ipsilateral motor cortex
   activity during unimanual hand movements relates to task complexity. *Journal of neurophysiology*, 93(3), 1209–1222.
- Verstynen T.D., Phillips J., Braun E., Workman B., Schunn C., Schneider W. (2012) Dynamic
   Sensorimotor Planning during Long-Term Sequence Learning : The Role of Variability,
   Response Chunking and Planning Errors. *PLoS One* 7:e47336.
- Verwey W.B. (1996). Buffer loading and chunking in sequential keypressing. Journal of
   *Experimental Psychology: Human Perception and Performance*, 22(3):544–562.

- Walther A., Nili H., Ejaz N., Alink A., Kriegeskorte N., Diedrichsen J. (2015). Reliability of
   dissimilarity measures for multi-voxel pattern analysis. *Neuroimage*, 137, 188-200.
- Wiestler T., Diedrichsen J. (2013). Skill learning strengthens cortical representations of motor
   sequences. *eLife*, 2013:1–20.
- Wong, A. L., Lindquist, M. A., Haith, A. M., & Krakauer, J. W. (2015). Explicit knowledge
   enhances motor vigor and performance: motivation versus practice in sequence tasks.
   *Journal of Neurophysiology*, 114(1), 219-232.
- Wymbs N.F., Bassett D.S., Mucha P.J., Porter M.A., Grafton S.T. (2012). Differential
   recruitment of the sensorimotor putamen and frontoparietal cortex during motor chunking in
   humans. *Neuron*, 74(5), 936–946.
- Yokoi A, Diedrichsen J. 2017. Does human primary motor cortex represent sequences of finger
   movements? bioRxiv, 157438
- Yousry T.A., Schmid U.D., Alkadhi H., Schmidt D., Peraud A., Buettner A., Winkler P. (1997)
   Localization of the motor hand area to a knob on the precentral gyrus. A new landmark.
   *Brain: a journal of neurology*, 120(1), 141–157.

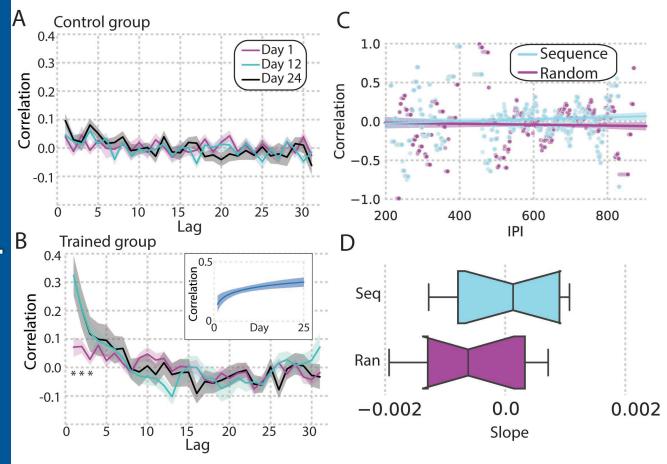
# **JNeurosci Accepted Manuscript**





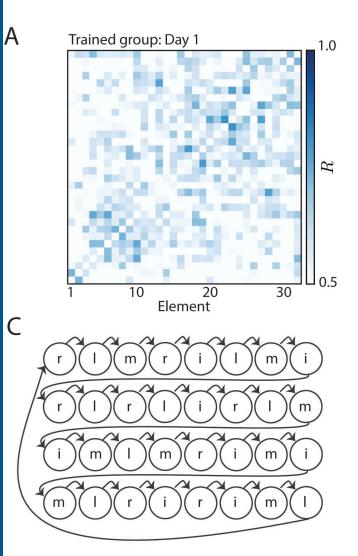


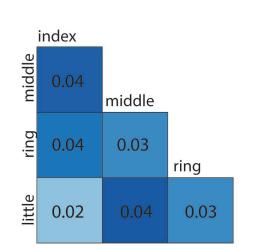
# **JNeurosci Accepted Manuscript**

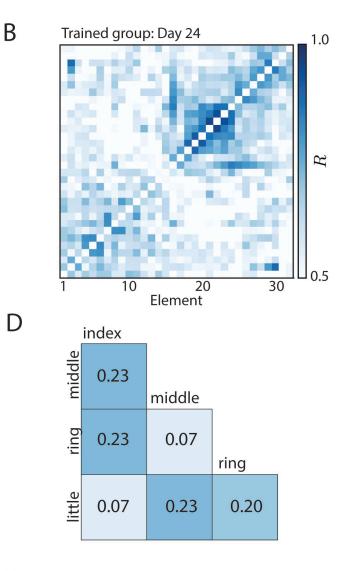


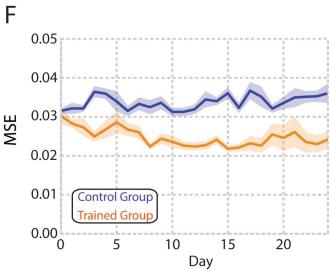


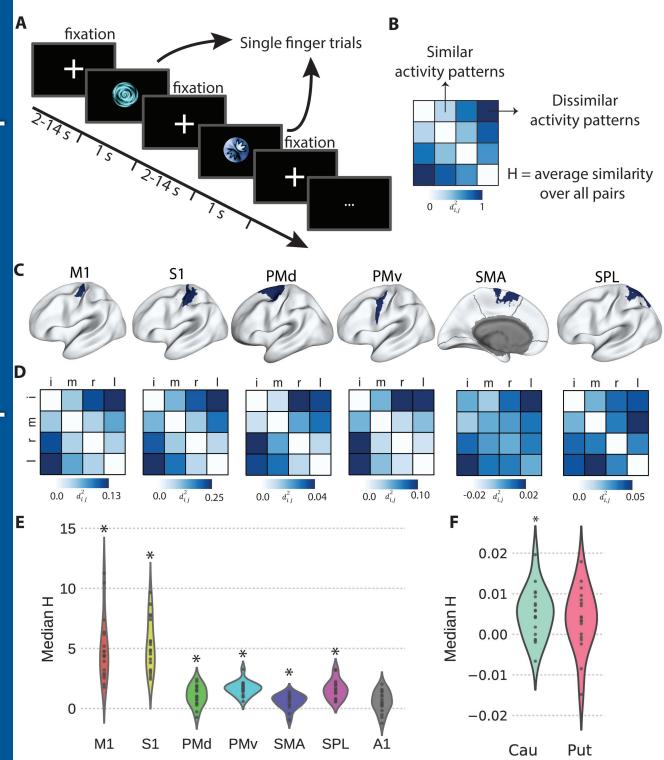
Е











**JNeurosci Accepted Manuscript** 

# <u>JNeurosci Accepted Manuscript</u>

